AD-A113 500 NAVAL RESEARCH LAB WASHINGTON DC F/G 14/5
NON-DESTRUCTIVE EVALUATION OF DEFECTS IN STRUCTURAL MATERIALS U--ETC(U)
APR 82 M FATEMI, B B RATH
UNCLASSIFIED NRL-MR-4749 NL

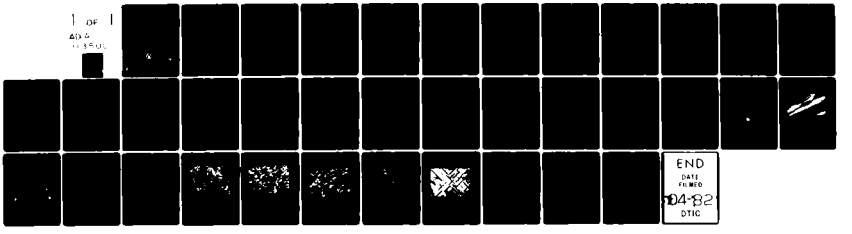

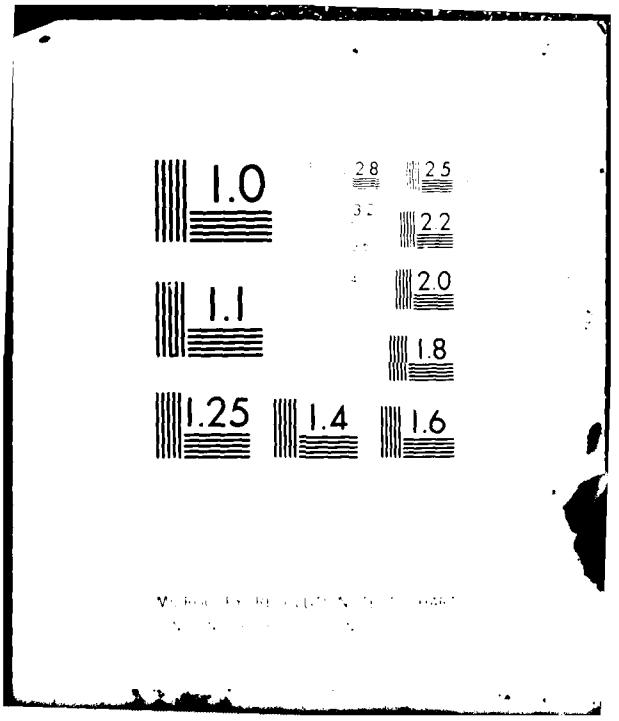
1.0
2.8
2.5
2.2
1.1
2.0
1.8
1.25
1.4
1.6

NRL Memorandum Report 4749

Non-Destructive Evaluation of Defects in Structural Materials Using Long-Wavelength Neutrons

Third Annual Report

M. FATEMI AND S. S. RAO

Physical Metallurgy Branch
Material Science and Technology Division

April 2, 1982

SECURITY CLASSIFICATION OF THIS PAGE (When Data Entered)

REPORT DOCUMENTATION PAGE	READ INSTRUCTIONS BEFORE COMPLETING FORM
1. REPORT NUMBER: NRL Memorandum Report 4749 — 2. GOVT ACCESSION NO.: AD-A113 572	3. RECIPIENT'S CATALOG NUMBER
4. TITLE (and Subtitle): NON-DESTRUCTIVE EVALUATION OF DEFECTS IN STRUCTURAL MATERIALS USING LONG-WAVELENGTH NEUTRONS — THIRD ANNUAL REPORT	5. TYPE OF REPORT & PERIOD COVERED: 3rd Annual report Nov. 1980 — Dec. 1981
	6. PERFORMING ORG. REPORT NUMBER
7. AUTHOR(s): M. Fatemi and B.B. Rath	8. CONTRACT OR GRANT NUMBER(s)
9. PERFORMING ORGANIZATION NAME AND ADDRESS: Naval Research Laboratory Washington, DC 20375	10. PROGRAM ELEMENT, PROJECT, TASK AREA & WORK UNIT NUMBERS: 61153N; 63-1073-0-0
11. CONTROLLING OFFICE NAME AND ADDRESS: Office of Naval Research Arlington, VA 22217	12. REPORT DATE: April 2, 1982
	13. NUMBER OF PAGES: 36
14. MONITORING AGENCY NAME & ADDRESS(if different from Controlling Office)	15. SECURITY CLASS. (of this report): UNCLASSIFIED
	15a. DECLASSIFICATION/DOWNGRADING SCHEDULE

16. DISTRIBUTION STATEMENT (of this Report)

Approved for public release; distribution unlimited.

17. DISTRIBUTION STATEMENT (of the abstract entered in Block 20, if different from Report)

18. SUPPLEMENTARY NOTES

19. KEY WORDS (Continue on reverse side if necessary and identify by block number)

Non-destructive testing
Small angle neutron scattering
G.P. zones
Voids
Powder metallurgy

20. ABSTRACT (Continue on reverse side if necessary and identify by block number)

Small-angle neutron scattering (SANS) measurements have been performed on several structural alloys to study voids and microporosities in powder consolidates of Al- and Fe-base alloys. The evolution of precipitates in Al-4%Cu and in beta-III Ti (Ti-11Mo-7Zr-5Sn-0.08Fe-.015C-0.012-0.1O) alloys subjected to varying annealing temperatures and times, and the nucleation and growth of voids formed during creep and superplastic forming in (Cu-3Al-2Si-.5Zn-0.4Co) alloys.

(Continues)

DD FORM 1 JAN 73 1473 EDITION OF 1 NOV 65 IS OBSOLETE
S/N 0102-014-6601

SECURITY CLASSIFICATION OF THIS PAGE (When Data Entered)

20. ABSTRACT (Continued)

The θ'' to θ' phase transformation in Al-4%Cu has been measured and analyzed. Calculated size density distributions show the coarsening of θ' phase with simultaneous disappearance of θ'' as a function of annealing times at 190°C. From these observations, the average size of precipitates at each stage has been calculated and compared with electron micrographic results. Similarly the precipitation of omega-phase in beta-III titanium has been observed for several annealing temperatures (600°F to 800°F) and aging times (2 min. to 100 hrs.). The observation of pronounced peaks in the small-angle profiles leads to an evaluation of the coherence length resulting from a clustering of precipitates. Comparison with TEM observations shows good agreement with SANS analysis.

Microporosity in powder consolidates has been studied in two alloys: (Fe-21Cr-6Ni-9Mn-0.02C-0.25N (Wt%)) and Ti-6Al-4V. The results have been analyzed using Guinier formulations. The analysis shows a variation of Guinier slopes consistent with the expectations of pore size and density variation as a function of the compaction pressure and temperature.

Finally, preliminary measurements on superplastically deformed alloys of (Cu-3Al-2Si-.5Zn-.4Co) have been made under varying conditions of strain and strain rates to determine creep-induced void densities. These data indicate an increase in the scattering profile intensities consistent with the above parameters. Because of the observed low density of voids, however, more refined measurements are in progress.

CONTENTS

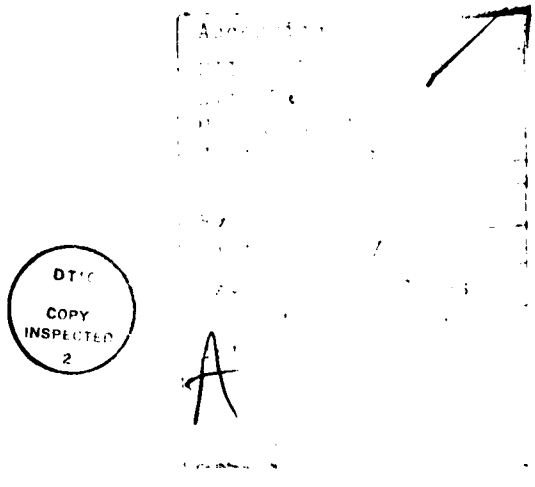

PREFACE

The Naval Research Laboratory (NRL) submits this progress report and work statement to the Office of Naval Research for continued research in small-angle neutron scattering (SANS) applications to defect evaluation in structural materials. The study will be conducted by NRL scientists using the SANS facility at the National Bureau of Standards (NBS) and at the Oak Ridge National Laboratory (ONL). The overall program objective of this research is to non-destructively evaluate nucleation and growth of voids formed during creep and superplastic forming, determine microporosity in powder consolidates, fatigue and fatigue/creep-induced microcracks in structural alloys, and characterize precipitation and second-phase embrittlement in high-temperature alloys and ceramics.

The program goal is to provide a new non-destructive test method with appropriate standardization in specific Naval structures such as superplastically deformed/diffusion bonded structures, powder consolidates of compressor and turbine blades. The program research for ONR support will consist of a systematic evaluation of the formation of voids at grain boundaries and grain edges of superplastic alloys, subjected to varing strain rates, stress and temperature. This ONR supported program will complement the ongoing NRL research on the non-destructive evaluation of size and distribution of precipitates in Fe-base alloys.

Additionally, the program will closely interact with two ONR research contracts at the University of Utah and Carnegie Mellon University.

Requests for additional information pertaining to this report will be welcomed by the following NRL representatives:

Dr. B. B. Rath	767-2465
Dr. M. Fatemi	767-2925

NON-DESTRUCTIVE EVALUATION OF DEFECTS IN STRUCTURAL MATERIALS USING LONG-WAVELENGTH NEUTRONS

INTRODUCTION

The application of non-destructive test methods to the problem of evaluating microstructural defects in materials has been a subject of ever increasing importance in materials science. To a large extent, this trend is due to the development of engineering materials of sophisticated composition aimed at higher durability and performance. It has been previously indicated (1-3) that, the possible choices for the types of non-destructive analysis on different materials have been limited. Small-angle neutron scattering (SANS) was considered as one of the most appropriate for flaw detection in bulk materials, where defects of interest were commonly in the form of voids and/or precipitates in a size range of approximately 100-1000 angstroms.

The intensity profile of small angle scattering as a function of angle is generally a monotonically decreasing quantity, and contains information on the size and number density of the scattering centers in that material. When, for example, two samples of identical microstructure and composition are compared by small angle scattering, (one of which contains the said defects) the relative difference in the respective scattering curves is directly relatable to the defect content in the sample. Furthermore, the shape of the net scattering curve, obtained from the differences between the two intensities, can be analyzed to evaluate a relative size distribution of the defects.

The ultimate purpose for SANS measurements is to derive information in a non-destructive manner pertaining to such parameters as the average defects size, their distribution, and the time-evolution of defects when the host

Manuscript submitted January 11, 1982.

material is subjected to varying thermomechanical treatments. To accomplish this purpose, particle size distribution techniques are devised. These calculations are usually based upon the inversion of an integral, the integrand of which consists of a product of the size-distribution function and the single particle intensity function. Numerical calculations are necessary, since there are no universal, closed, analytical forms which can be used to define the scattering profiles of different samples and materials. Although, in principle, it should be possible to write an exact numerical program, which could be used for all scattering curves, the actual execution of such a program would be nearly impossible. Any size distribution calculation, therefore, requires certain restrictions as well as major and minor assumptions relating to the shape, background level, interference and geometrical effects.

The SANS study in this investigation has been directed as a non-destructive test method to evaluate size distribution of precipitates and voids too small to be identified by any other existing NDE methodology. Several investigators have attempted with the use of different algorithms to derive size distributions from SANS profiles (4-7). Most of them used solutions of an integral equation of the type:

$$I(q) = K\int_0^\infty D(R)m^2(R)I_o(qR)dR \qquad (1)$$

which relates the density D(R) of particles of radius R to the measured integrated intensity I(q). In the above equation $q = 4\pi \sin\theta/\lambda$, m is the excess nuclear scattering length density in the particle and $I_o(qR)$ is the single particle scattering function which depends on the particle shape and dimensions.

Experience has shown that most scattering data may be analyzed with the aid of an appropriate size distribution algorithm using inversion of the

intensity integral. There are, however, a few cases where such an analysis is either difficult or unnecessary. The major difficulties arise from situations where the intensity data is limited to fairly small scattering angles, beyond which statistical errors are too large to render the data meaningful. Since the intensity integral provides meaningful distributions only when evaluated over a wide range of scattering angles, it is possible to extend the scattering data to larger angles under reasonable mathematical assumptions or longer measurements and then use the expanded data for size distribution analysis. However, the accuracy of this approach is strongly dependent upon the description given to the complete scattering profile.

A second approach to the analysis of scattering profile is available which does not require size distribution analysis by inversion. When a sample contains a uniform dispersion of nearly similar particl sizes, the measurement gives rise to a scattering curve which, when analyzed for size distribution, would ideally correspond to a narrow particle size range. For these situations, data can be analyzed using the procedure proposed by Guinier (8) which linearly relates the natural logarithm of intensity (lnI) to the square of the wave-vector (q^2). The slope of such a plot is related to the particle size through the relationship:

$$\text{slope} = \frac{\Delta \ln I}{\Delta(q^2)} = -\frac{R^2}{3}$$

where R is the radius of gyration of the spherical particles. Thus, a relatively quick way of ascertaining the type of particle size distribution in the sample is to use the Guinier analysis. If it exhibits a straight-line behavior between lnI vs. q^2 over a significant portion of the small-angle scattering, it is an indication of nearly uniform size particles. If, on the other hand, it shows a trend of varying slopes, either particles of

varying size and distribution or other complex scattering interactions may be present. If the presence of a widely varying particle or void size distribution is recognized from other independent observations, a more elaborate size distribution calculation is warranted.

PROGRESS

Major accomplishments during the last fiscal year were: (1) observation and analysis of microporosity in powder consolidated stainless steels compacted under varying temperatures, ranging between 800°C and 1200°C; (2) SANS observation of the effect of HIP pressure on Ti-6-Al-4V powder compacted alloys; (3) preliminary measurements on voids generated in (Cu-3Al-2Si-0.5Zn-0.4Co) alloys superplastically deformed at varying strains and strain rates; and (4) evaluation of the G.P. zone formation by SANS in Al-4% Cu alloys. A detailed description of these measurements is presented in the following sections.

1. Porosity in Powder Compacted Stainless Steels

1A. Expermental. Samples of stainless steel (Fe-21Cr-6Ni-9Mn-.02C-.25N_2, wt%), were obtained from Sandia Corporation. Table I lists sample designations and characteristics.

For SANS measurements all samples were ground to the thickness of 2.5mm (nominal). Surfaces were polished on 400 and 600 paper, then finished by Linde A to remove all grinding scratches and deformation. A standardized sample preparation procedure was adopted to ensure uniformity and a minimization of surface strain. Minor variations in surface conditions have been shown to affect small-angle scattering profile (9).

Neutron scattering measurements were performed at ORNL SANS facility. Following a few preliminary measurements, it was established that most scattering was confined to very small angles ($q = .005$ to $0.015A^{-1}$). The

sample-to-detector distance was thus set at 16 meters for improved resolution on the 64 x 64 element position-sensitive detector. The measurement time for each sample was about 1-1/2 hours. This included the time for transmission measurements, and evacuation of the sample chamber. The scattering characteristics of a standard sample (wrought stainless steel) were measured and substracted from each of the samples to obtain a true measure of the scattering attributable to defects. Data processing included the correction of data background measurements and normalization of all data by the transmission and thickness factors, similar to the method described in the previous reports. A typical isointensity plot on 64 x 64 grid is shown in Fig. 1.

1B. Analysis. The Guinier plots from SANS measurements are shown in Fig. 2. Several important features of these measurements can be seen by comparing various samples in terms of temperature and density.

For clarity in the display, two different scales are used; the lower from q=0 to $q=8x10^{-4},A^{-2}$, the upper from q=0 to $q=2x10^{-4},A^{-2}$. The upper set shows the detailed variation in the maximum pore size, (corresponding to low-q measurements), while the lower set indicates the relative intensity of the smaller particles (related to higher-q measurements).

It is clear that the overall sample scattering decreases with increasing temperature. Furthermore, the relative density quoted in Table I appears to be directly related to the temperature, such that the lowest temperature (800°C) corresponds to the lowest density (98.9%) and the highest temperature (1200°C) to the highest density (99.8). The difference in scattering between these two extreme cases, which is larger than one order of magnitude, is consistent with the picture of voids as the major source of scattering.

Furthermore, the slope of each curve, characterizing its shape, gives information about relative pore sizes. Thus, B36 gives a larger maximum pore size compared to all other samples, while its overall density of pores is probably somewhat less than B33-34, both of which have nearly the same measured density of 99.3%.

There is some degree of uncertainty in the quoted densities, but it is clear that there is at least a strong suggestion of some systematic variation of density with temperature. An attempt is presently being made to evaluate the density of these materials independently of earlier measurements.

Based on the observations mentioned above, the relatively low overall scattering intensity (*after subtraction of intensity from standard*) indicates low pore densities. Assuming that pores of an average size of 500Å (0.05μm) are present, a simple calculation of their number on the basis of the given weight density yields a value of about 10^{13} voids/cm^3. This number may be converted to a surface density distribution appropriate for observation by SEM or similar techniques. Based on this conversion the calculated spacing corresponding to the above void density will be about .5 μm (5000Å) between the voids for the material of relative density of 99.8%. Observations of these voids by SEM proved difficult because the void size was of the same magnitude as the surface irregularities in the specimen. Figure 3 shows typical SEM micrograhs obtained from one of the samples (A6). These micrographs indicate the uncertainties in the interpretation of voids and their lack of distinction from surface irregularities.

Direct observation of voids using transmission electron microscopy was performed for several selected samples. This procedure is not without difficulty because the voids exposed to the surface are enlarged by the electrothinning processes and therefore contribute to an error in the size distribution analysis. However, the interior voids remain unaffected and can provide a good estimate of number density and size.

Figures 4, 5, and 6 demonstrate the use of three TEM methods used in the observation of voids for sample B28. In Fig. 4, the specimen is set at S=0 (exact Bragg condition), where S is the deviation for Bragg angle. Interference fringes from variation of sample thickness are observed. Here, the intensity contrast from voids changes alternately from white to black to white. The method is thus suitable for observation of small voids. In this micrograph voids of a size range mostly in 100-400 Å, plus a very large hole (~3000Å) are visible.

In Fig. 5, a multibeam condition with S≠0, larger voids (approximately 700 Å) are visible.

Figure 6, (with large S) is a two-beam condition (weak beam), which permits delineation of the void (shown by the arrow) together with excellent resolution of dislocation line images.

In order to minimize the adverse effects of electrothinning, a new procedure consisting of electropolishing followed by ion-milling (a minimum of 1h to remove first few hundred angstrom layer from the surface) is being developed.

2. Porosity in HIPed Ti-6Al-4V

2A. Experimental. Three samples of HIP-Ti-6-4 were supplied by Gould Corp. Titanium alloy powder was consolidated in autoclave at a temperature of 1275°C and at pressures of 60, 80, and 100 ksi, respectively. The samples

and a standard Ti-6-4 were ground to a thickness of approx. 3.3mm, then polished on No. 400 and No. 600 Emery paper. As in the preceeding case, it was found that the longer sample-to-detector distance of 16 m was better suited due to the absence of significant data at larger scattering angles.

2B. Analysis. An analysis of pore sizes gives a range of values for D from 300Å at one extreme to 1150, 1020 and 880Å at the other extreme for 60, 80, and 100 ksi, respectively. Similary, it may be seen that the magnitude of scattering increases by about 100% at the higher angles for 80 and 100 ksi (compared to 60 ksi). However, at very small angles the scattering intensities from the 30 tsi sample exceed those from the others. This is shown in Fig. 7. This behavior indicates a refinement of pores with increasing pressure, and is again consistent with the effect of compaction pressure on pore size.

3. Phase Transformation in Al-4Wt% Cu

The investigation of the precipitation of Guinier-Preston (G.P.) zones in Al-4Wt% Cu alloys was carried out in order to 1) establish an important aspect of the SANS studies, namely, the applicability of the size distribution calculation to a wide range of sizes encountered in the same specimen which has undergone a change of internal microstructure upon heat treatment, and 2) provide a corroborative and yet non-destructive method to such other techniques as TEM, small-angle x-ray scattering, diffuse x-ray scattering, and SEM.

Precipitation in Al-4Wt% Cu is a complex process which must be analyzed under a variety of experimental conditions so that the effect of various phases on SANS profiles may be distinguished (10). In view of this complexity, the present study was limited only to an annealing temperature of 190°C, which is above the G.P. solvus and provides for the formation of two of the four possible phases; θ'' and θ'.

3A. Experimental. The sequence of phase transformation in Al-4%Cu is listed in Table II. The first precipitate appearing from solid solution is the well known G.P. (GP1) zone, observed earlier independently by Guinier and Preston (11).

It has been established that these zones consist of very fine plate-like structures (approximately 40-50Å in size) produced by segregation of Cu atoms to (100) planes of Al. The second zone is the so-called GP2 or θ" zone with a tetragonal structure. Following this transformation at about 190°C, the θ" disolves and in time gives rise to a CaF_2 structure of θ'. Finally, the coarser θ-phase, with a tetragonal structure is generated, and is coarsened in time. Figures 8 to 12 show the microsructures of these precipitates.

3B. Analysis. The SANS profiles of five samples annealed at 190°C for 3, 8, 24, 96, and 288 hrs respectively are shown in Fig. 13. The distinct difference between any two of these profiles indicates the variation in microstructure with regard to size and/or shape of defects. The profiles may be analyzed for size-distribution of the defects, although the qualitative outcome of such analysis may be judged from visual examination of the intensity plots. For example, the microstructure of the 8-hr sample is somewhat finer than that of the 3-hr sample as evidenced by the presence of larger wide angle component and smaller low-angle intensities. Similarly, the 24 hr data displays considerable high-angle scattering, and, when "dropped" to the same scale as the previous samples, shows comparatively lower small-angle component, indicating a refinement of particle sizes. Conversely, the samples at 96 and 288 hrs exhibit an entirely different behavior due to the increased ratio of small-angle to wide-angle components. indicative of much coarser particle sizes.

The calculated values of size distribution on these five samples are in agreement with the above inference. These results are shown in Fig. 14 and summarized in Table II, in terms of the breadth and average particle size.

Based on prior observation of these phases it may be seen that the refinement of particle in the first half of the annealing sequence is due to a gradual dissolution of the θ'' with concurrent appearance of the θ' phase, while the later coarsening at 96 and 288 hr is characteristic of θ'-growth.

This analysis of a rather complicated system has demonstrated quite clearly that SANS can be applied as a convenient method to follow the changes in the microstructure of an alloy in a non-destructive manner.

4. SANS Measurements in superplastically Deformed Cu-3Wt% Al Alloy.

The effects of strain and strain rate on nucleation and growth of voids in Cu alloy have been considered by several authors (12-14) and reviewed by Gunier (9). However, the observation of such voids has been limited to the range suitable for optical micrography, i.e., to voids in the range of 1 to 10 μm. The objective of the present work is to investigate the applicability of the SANS technique to the detection of voids during the early stages of their formation, where the size is about a few hundred angstroms.

4A. Experimental. Under superplastic and near superplastic conditions the maximum strain to fracture for Cu alloy was measured for several samples on an MTS machine equipped with a double split 3 zone furnace. The strain was found to be about 300%-400% at temperature of 550°C with an initial grain size of about 2-5 μm. For the purpose of a systematic SANS measurement, it was necessary to have samples of reasonable size with a uniform distribution of internal defects. Elongations to several 100% were found too high for this purpose because necking invariably occurred after about 50-100% maximum

strain. Furthermore, higher strains were not intended for these SANS tests because much larger voids than could be detected by SANS would have been generated. Sample preparation for such a study proved to be critical because of the requirements of very uniform hot zone covering the entire length of the elongated sample. It was necessary to start with relatively large sample dimensions before elongation in order to obtain sizable samples after elongation for SANS measurements. Since it is difficult to prepare large samples with uniform cross section, optimum sample sizes were required and a compromise had to be made between the possible and desirable dimension. The final sample configuration was chosen with a gauge section length of 3.8 cm and cross sectional area of 0.2 cm^2. In actual practice, samples were prepared in such a way that following the elongation, material of sufficient width and thickness was available for neutron scattering measurements. This implied, in addition to the need of maintaining uniformity of thermal profile as well as gauge dimension, that the starting pre-strain dimension be (1) large enough to yield a final sample of reasonable size, and (2) small enough to prevent plastic instability.

Samples were mounted on the MTS machine using a special "grip" with cut-outs which conformed to the curved shoulders of the specimens. The only necessary force retaining the samples was that supplied by tension, and thus the gauge region alone was deformed. This design allowed quick change of sample in a preheated double split furnance and also permitted the availability of a reference "unstressed" section from the same sample, having undergone an identical heat treatment. Initial calibrations were made to ascertain the uniformity of furnace temperature. For preliminary measurements, the following samples were prepared (Table III).

The measured strain rates given in Table III are the inital values calculated from cross-head speed and initial gauge length. The strain values were obtained by comparing the intial and final separation of fiducial marks made on the gauge region. About 30 such marks were made on each sample at a spacing of .050" before elongation. After completion of tests, the spacings were measured over the entire length, and those segments exhibiting uniform elongation were chosen for SANS measurements. Because of the relatively small thickness of the pieces, samples were sometimes stacked to obtain proper thickness suitable for neutron scattering. Final size of each SANS sample was about 8 x 10 x 3 mm thickness.

4B. SANS Measurement. Preliminary results were obtained from the superplastically deformed samples, (CD-5, CD-8, CD-11 and CD-12) and compared to a standard (unstrained). All data were normalized to a reference total incident neutron count and calibrated for thickness and transmission factors, so that a direct comparison from sample to sample could be made. Because of the small but finite difference between large scattering values from standard and deformed samples, an attempt was made to investigate the repeatability of the results in separate measurements. In two such trials, it was shown that (a) the standard scattering curve was consistent, and independent of the sample from which it was chosen, and (b) there was a consistent, repeatable difference between samples of different strain rate at the same strain. The latter point is discussed further.

The Guinier plots of the appropriate samples are shown in Fig. 15. To obtain these curves, the background-corrected normalized-data for each of the samples was smoothed, and the scattering profile from the standard was subtracted. The final result represented the scattering from the defects in the samples produced during deformation.

The most significant result was observed with regard to difference between the pairs of samples with equal strain but unequal strain rates: within each pair (CD-5 and CD-8; CD-11 and CD-12) the lower intensity profile corresponds to the higher strain rate, and vice versa. A comparison of the data also showed no discernible difference within the statistical limits, between CD-5 and CD-11 both of which have been represented in the figure by the same curve.

The overall shapes of the 3 final Guinier plots are quite similar. The maximum measureable R_g (radius of gyration) for these curves is about 580Å resulting in D_g (average cavity dimension) of about 1400Å while the lowest reliable dimension is D_g = 620Å. Due to the statistical limitations at lower intensities, it is difficult to determine the size of smallest defects. It may, however, be concluded from the low-q portion of the data, that defect density differs by a factor of 5 to 10 between the extreme samples, CD-12 and CD-8. On the other hand, comparing the pairs of samples with nearly equal strains, it is seen that higher strain rates gave rise to a lower overall defect density.

This behavior is in apparent disagreement with our earlier expectations, that the faster strain rates should have resulted in a larger number of defects. To ascertain the behavior of data at the lower intensities, measurements of longer time for wide scattering angles are being planned.

PROGRESS SUMMARY

The size and number densities of microvoids, precipitates and transformations in alloys have been non-destructively evaluated using long wavelength neutrons.

1. Microporosities in hot-isostatically compacted stainless steels were determined as a function of consolidation temperature. While at 1200°C, the pore density was at a minimum, the number of pores in the size range between 100 Å and 800 Å systematically increased with decreasing HIP temperature. These results are generally consistent with the measured densities of the consolidates. A more accurate density measurement is required before developing an appropriate empirical relationship.

2. A variation of compaction pressure on pore densities during hot-isostatic consolitation of Ti-6Al-4V powders were evaluated for a HIP temperature of 1275 °C. Consolidation voids were detected in all samples. The void sizes were refined with increasing HIP pressure.

3. A preliminary study was completed in determining the vacancy condensation void formation during superplastic deformation of a Cu alloy subjected to varying strains and strain rates. Void formation and growth was found to be sensitive to all deformation parameters and temperatures. The results suggest that the pore density goes through a maximum as a function of strain-rate. Higher strain rate contribute to a lower intensity profile indicative of a smaller volume fraction of voids in the alloy. Further investigation is needed to establish the strain-rate effects.

4. Precipitation in Al-4%Cu was investigated as a function of annealing time at 190°C. SANS results are shown to be in good agreement with electron microscopic evaluation of precipitate size and densities.

5. An investigation has been initiated to determine the evolution of delta-prime phase as a function of aging time in powder consolidates of Al-2.5Li-1Cu alloy. The strength and toughness related properties are shown to be dependent on the size and distribution of the second phase.

FUTURE PLANS - STATEMENT OF WORK

Preliminary investigation on the void formation in superplastically deformed alloys has revealed that micropores form nearly homogenously in an alloy during superplastic deformation, which is a sensitive function of strain, strain rate and temperature. Contrary to expectation, a superplastically deformed Cu-alloy shows lower pore density when strained at higher rates. The phenomenon of void formation is of increasing importance, because of the technological value of superplastic forming of titanium and iron alloys to near net-shapes in structural application.

The investigation using long-wavelength neutrons for evaluation of defects will be conducted under three tasks:

Task 1 will be directed to a systematic study of the effects of strain, strain rate, temperature and prior-microstructure on the nucleation and growth of voids in a Cu-base alloy. Supporting study using electron microscopy will establish the preferential sites for void nucleation leading to an understanding of the mechanism of void formation and the critical deformation parameters responsible for their nucleation and growth. Preliminary studies will be conducted using either titanium- or iron-base alloys. Room temperature fracture characteristics of the superplastically deformed alloys will be evaluated to determine the role of pre-existing voids in crack-formation and fracture.

Task 2 will be directed to evaluating consolidation voids in powder compacted alloys. Effects of consolidation temperature, pressure and time under hot-iostatic compression on the residual pore size and density will be evaluated in stainless steels, aluminum and titanium alloys. Preliminary results show the temperature effects on void densities in stainless steels.

In Task 3, NRL scientist will interact with ONR 6.1 research contractors in a collaborating effort to evaluate defects in metals and alloys.

During FY82, there will be two collaborative investigations. One will be with Prof. J. G. Byrne of the University of Utah to investigate the effects of hydrogen and heat-treatments on the blister formation in Cu-base alloys. Preliminary investigation has already been initiated for this investigation. The second program will consist of a systematic study of the nature of microcrack nucleation at the interface between the iron-alloy matrix and the second phase particles in the presence of applied stress and varying hydrogen concentration. A measure of defect density will help elucidate the mechanism of preferential segregation of hydrogen to the interface and the nature of hydrogen embrittlement of alloys.

Table I — Sample designations and processing temperatures for (21-6-9) stainless steel alloys. Compaction pressure = 15 ksi.

Sample #	Temp., °C	Density*
B26	800	98.7
B28	800	98.9
B27	900	99.5
B33	1000	99.5
B34	1000	99.2
B36	1100	99.3
A5	1200	99.6
A6	1200	99.8
STD		100.0

*Nominal density is measured relative to wrought material as 100.0.

Table II — Precipitation size distribution measured by SANS in Al-4Wt%Cu alloys annealed at 190°C

Annealing Time	Precipitate Peak Size	Width at 50% Peak Height	Remarks
3	400	950	θ"
8	360	850	θ" + θ'
24	100	75	θ'
96	109	170	θ' growth
288	243	520	θ' growth

Table III — Strain and strain-rate parameters for superplastically deformed CD-638 Cu-alloy samples. T = 550° C.

Sample id#	Strain (%)	Strain rate (/sec)
CD-4	25	0.1
CD-5	25	0.05
CD-6	20	0.3
CD-7	22	0.003
CD-8	25	1.2
CD-11	50	5.0
CD-12	55	0.01
CD-19	95	1.3
CD-30	60	0.15

Temp = 550°C

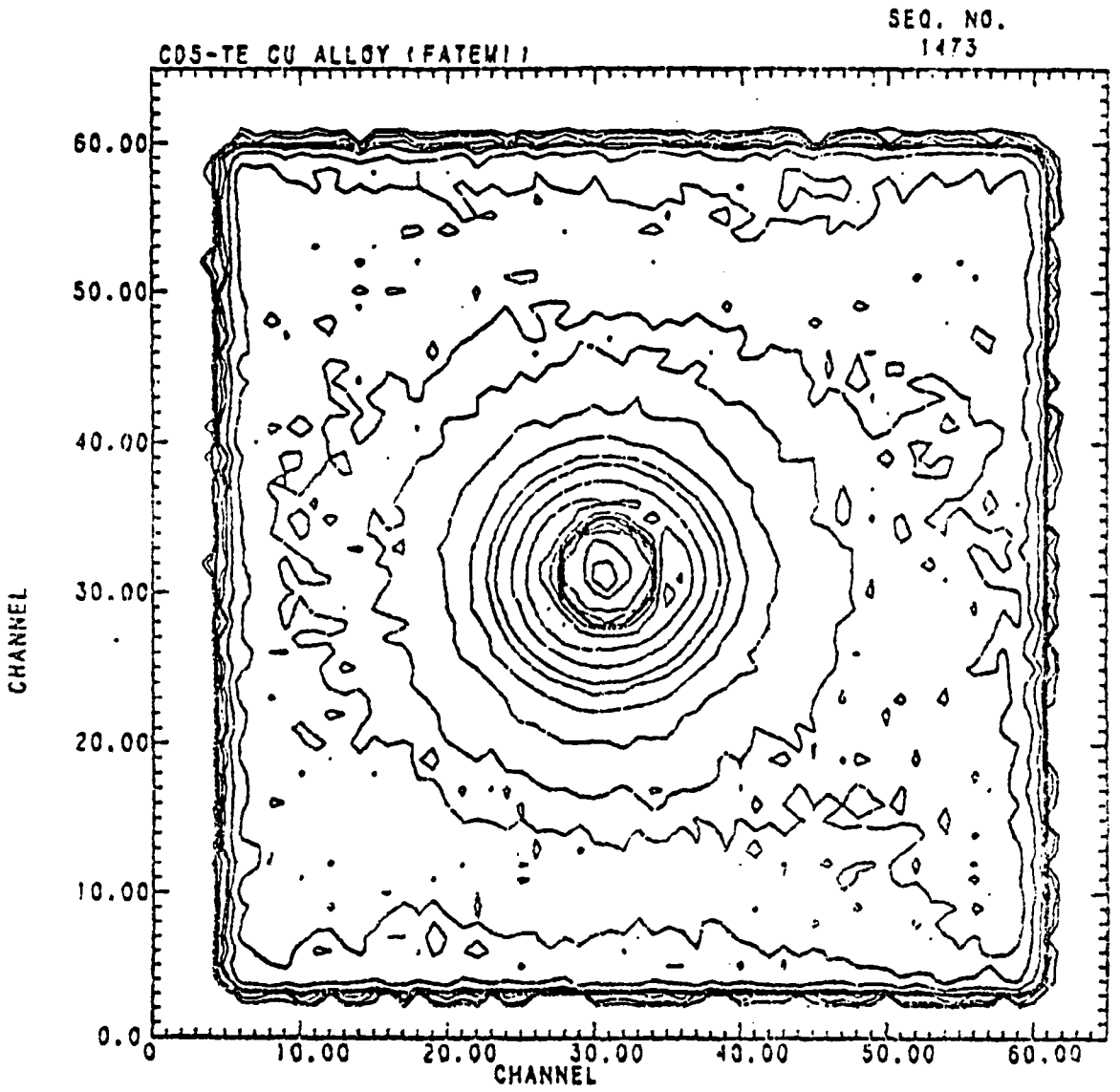

Fig. 1 — Typical isointensity contour plot obtained on a 64 × 64 cm area position — sensitive detector

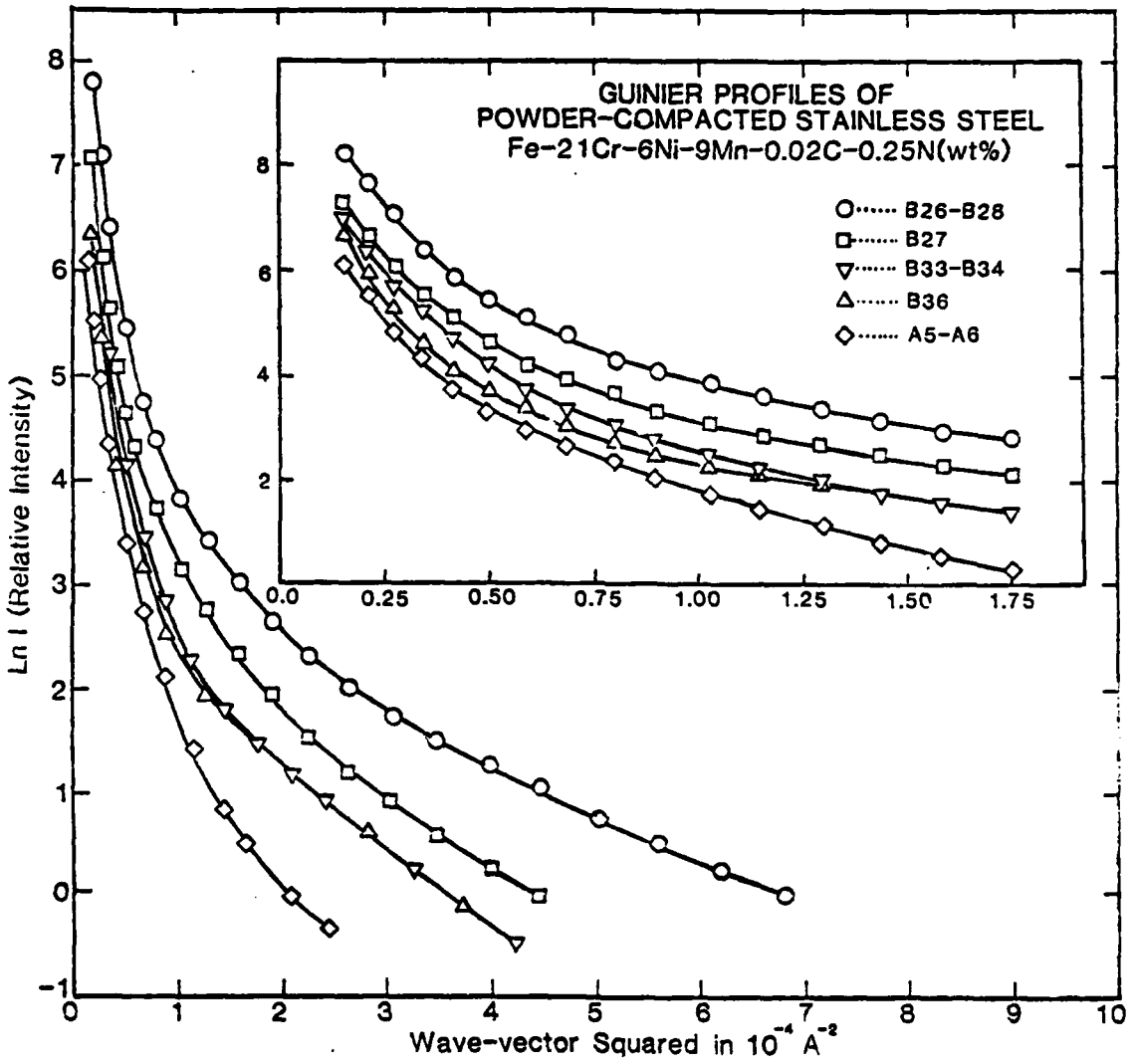

Fig. 2 — Guinier plot of SANS intensity profiles from (21-6-9) stainless steel showing the reduction of intensity with increased compaction temperatures from 800°C to 1200°C.

(a)

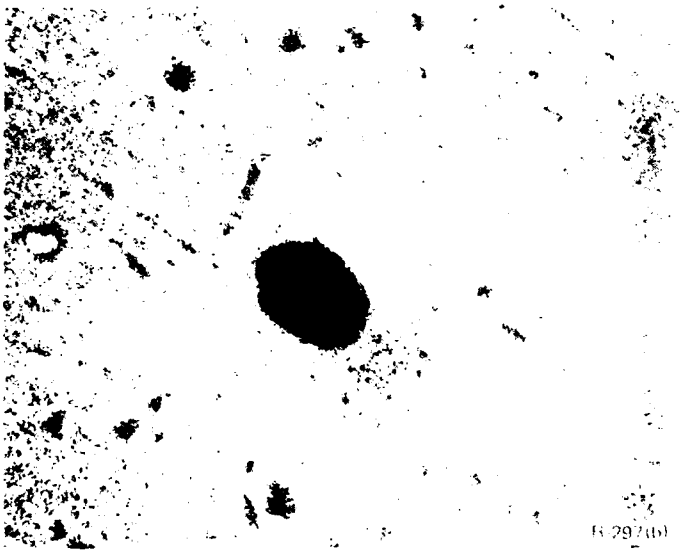

(b)

Fig. 3 — SEM micrographs of voids and surface irregularities in sample (A6). (a) Backscattering micrograph at 4KX, (b) Secondary-beam micrograph at 20 KX.

Fig. 4 — TEM micrograph of sample (B28) at 58,000X, showing interference thickness fringes and change of contrast for various voids

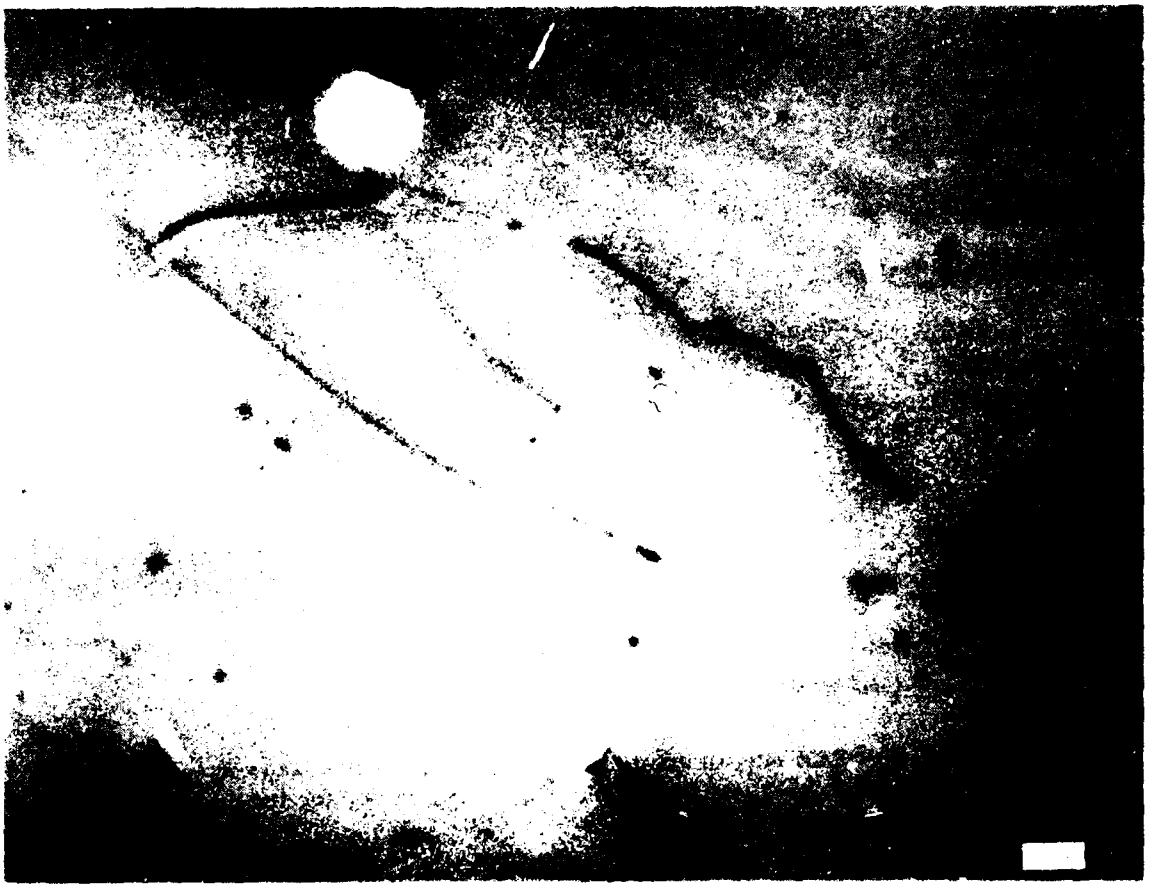

Fig. 5 — Multibeam TEM micrograph of sample (B28) at 145,000X

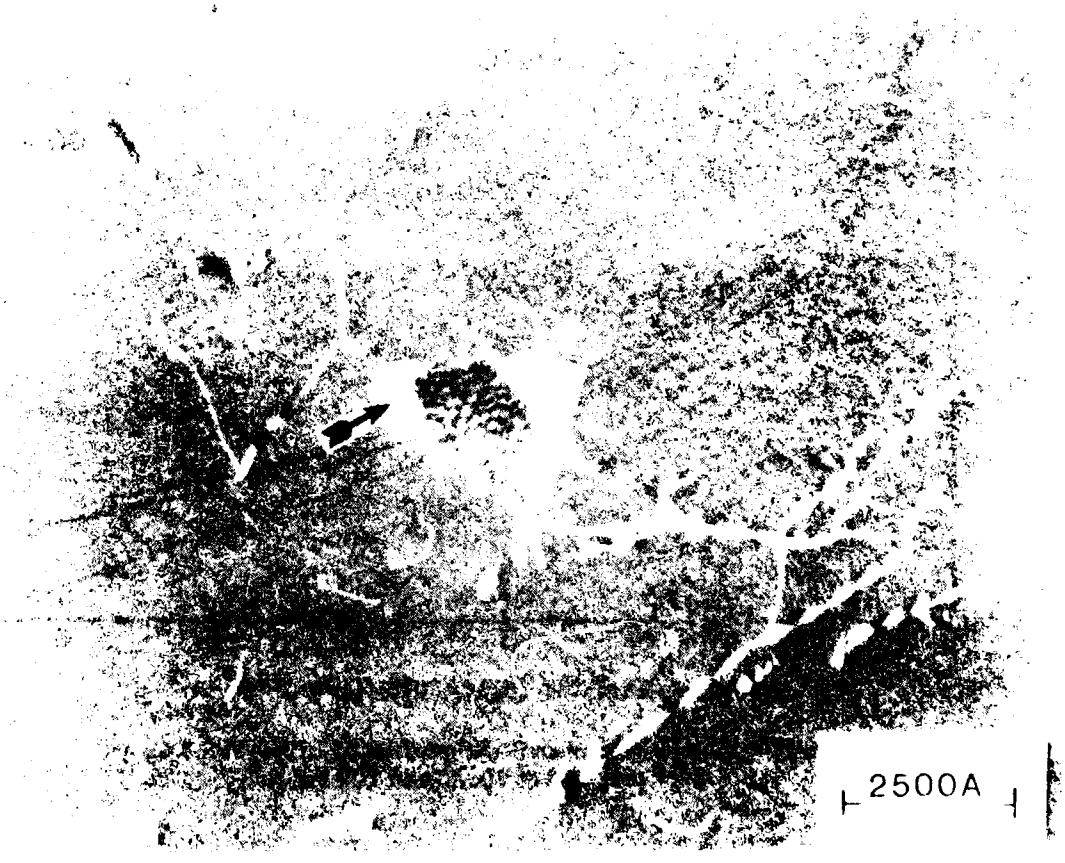

Fig. 6 — Weak-beam micrograph of B28 at 125,000X showing a void and related dislocation network

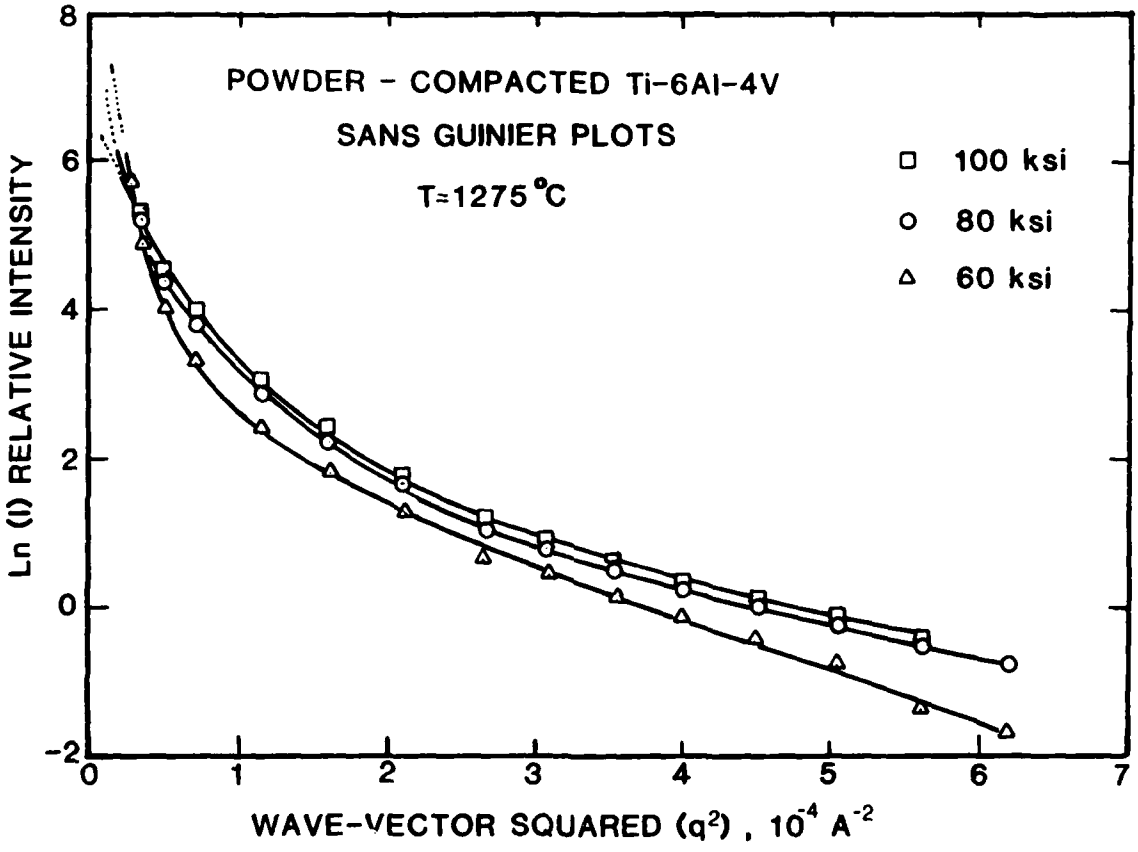

Fig. 7 — Guinier plot from SANS profiles of HIPed Ti-6-4 alloys prepared at 60, 80 and 100 ksi

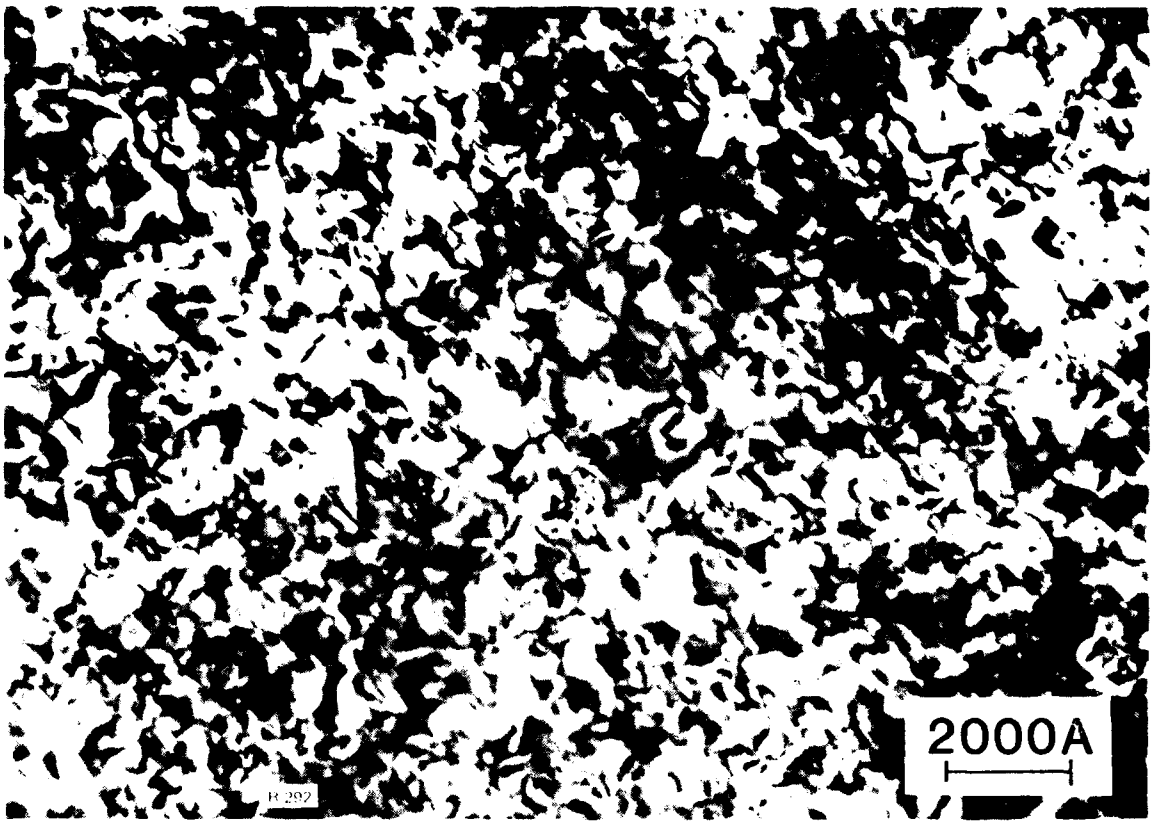

Fig. 8 — Transmission electron micrograph of Al-4Cu alloy, homogenized 16 hrs at 575°C, aged 3 hrs at 190°C showing θ'' precipitates.

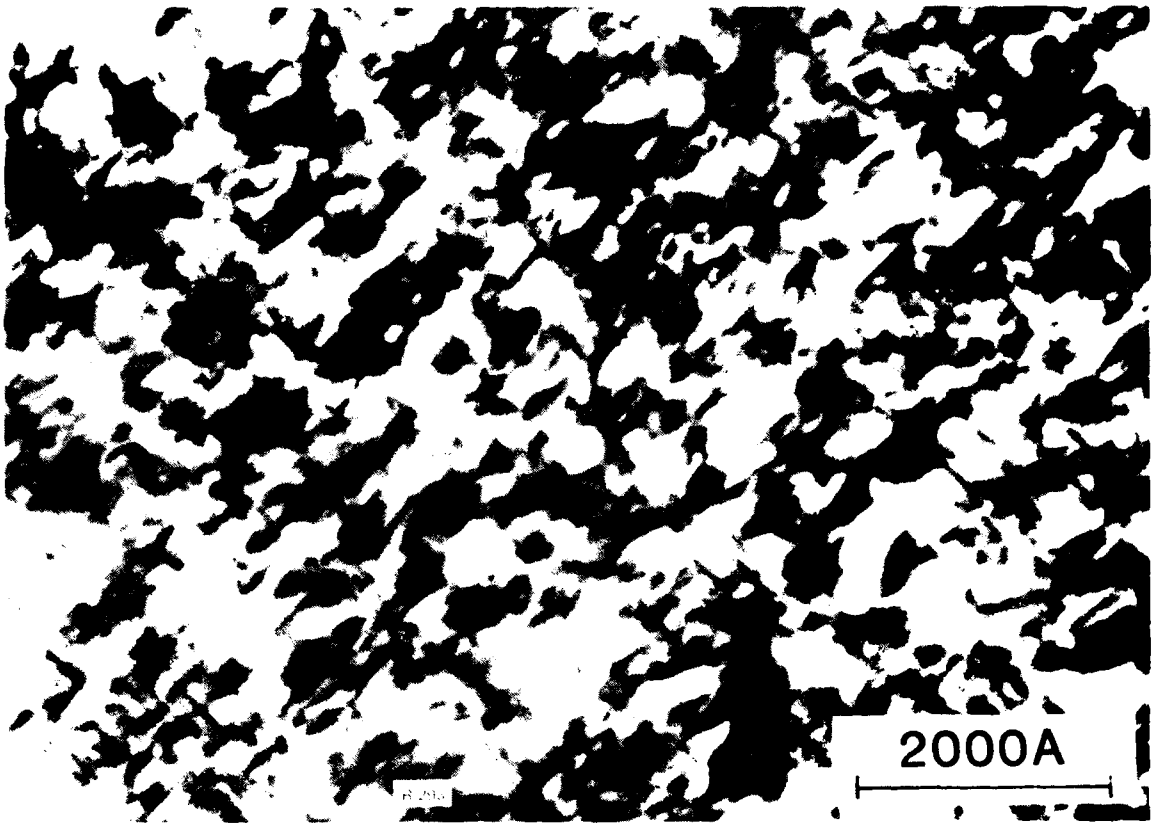

Fig. 9 — TEM micrograph of Al-4Cu, aged 8 hrs at 190°C showing θ'' and appearance of θ' precipitates

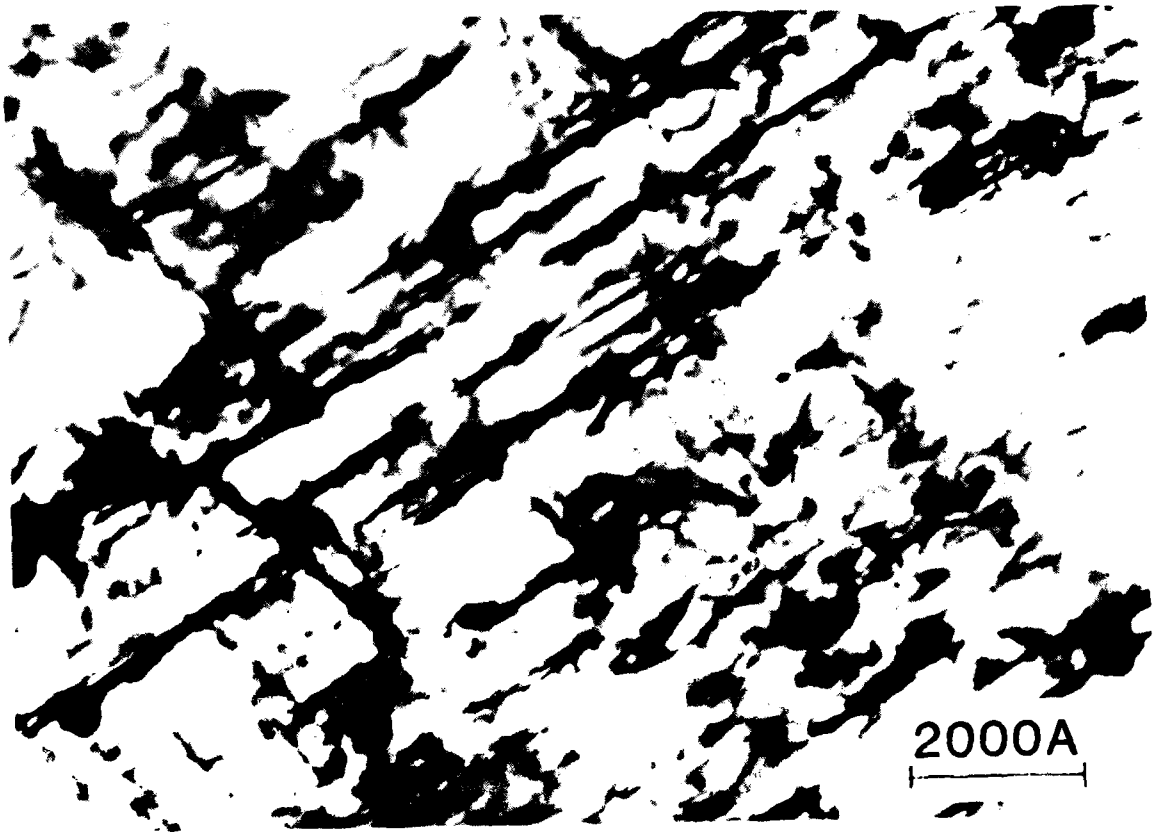

Fig. 10 — TEM micrograph of Al-4Cu, aged 24 hrs at 190°C showing mainly θ'

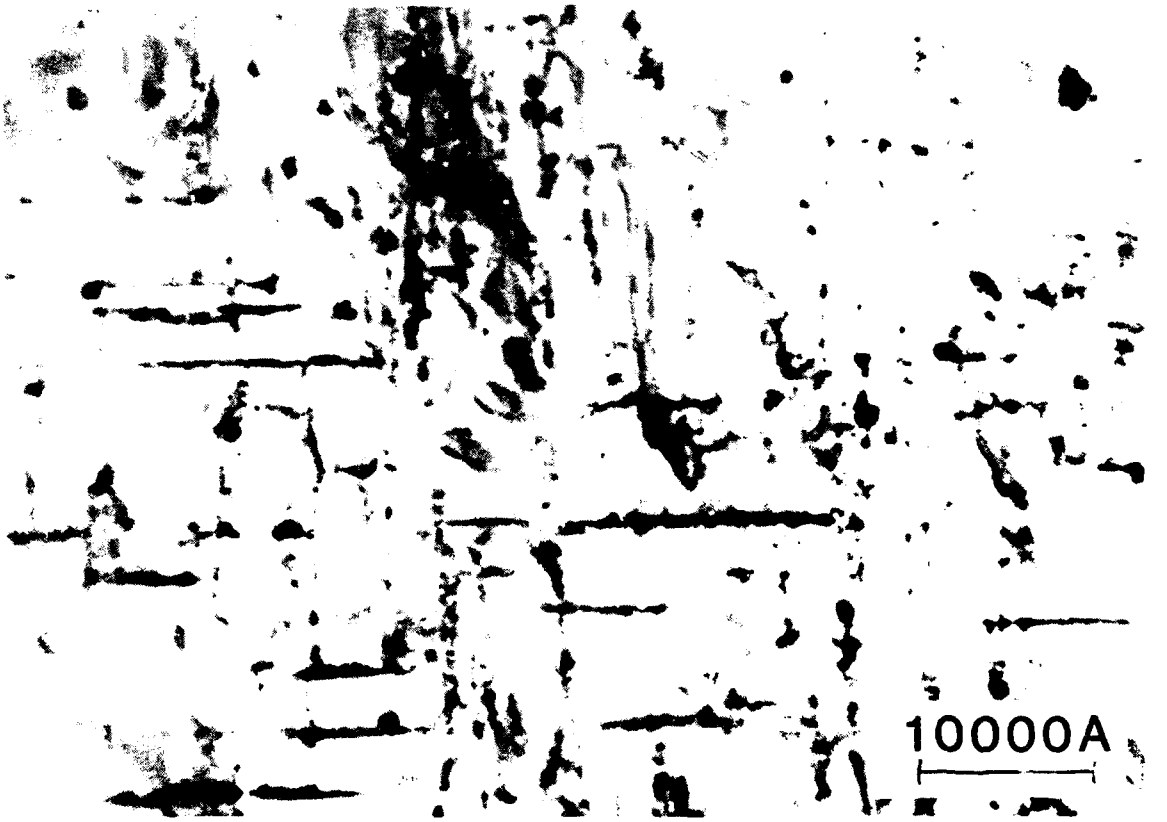

Fig. 11 — TEM micrograph of Al-4Cu, aged 96 hrs at 190°C, showing coarsening of θ'

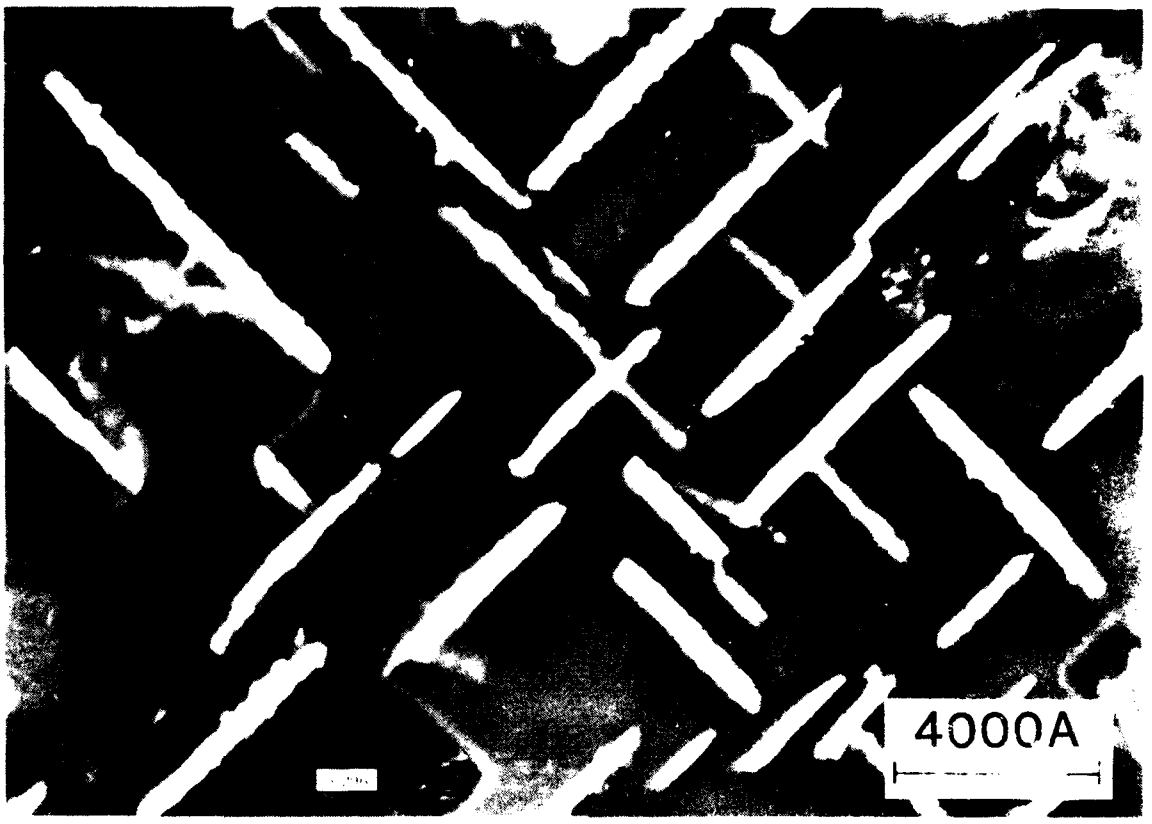

Fig. 12 — Dark field electron micrograph of Al-4Cu alloy, aged 288 hrs at 190° C showing enlarged θ' precipitates

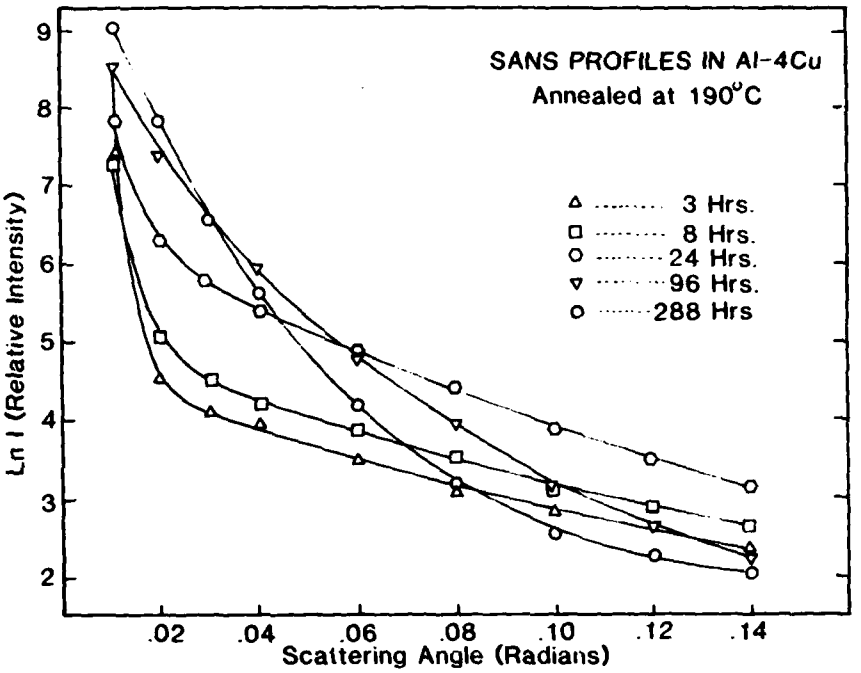

Fig. 13 — SANS intensity profiles of Al-4Cu samples aged from 3 to 288 hrs.

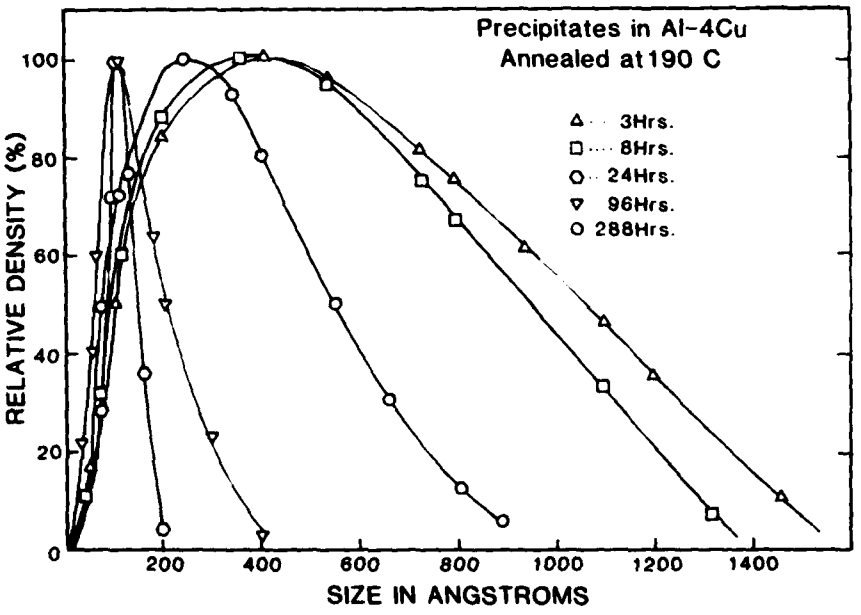

Fig. 14 — Calculated size distribution of precipitates in Al-4%Cu alloy

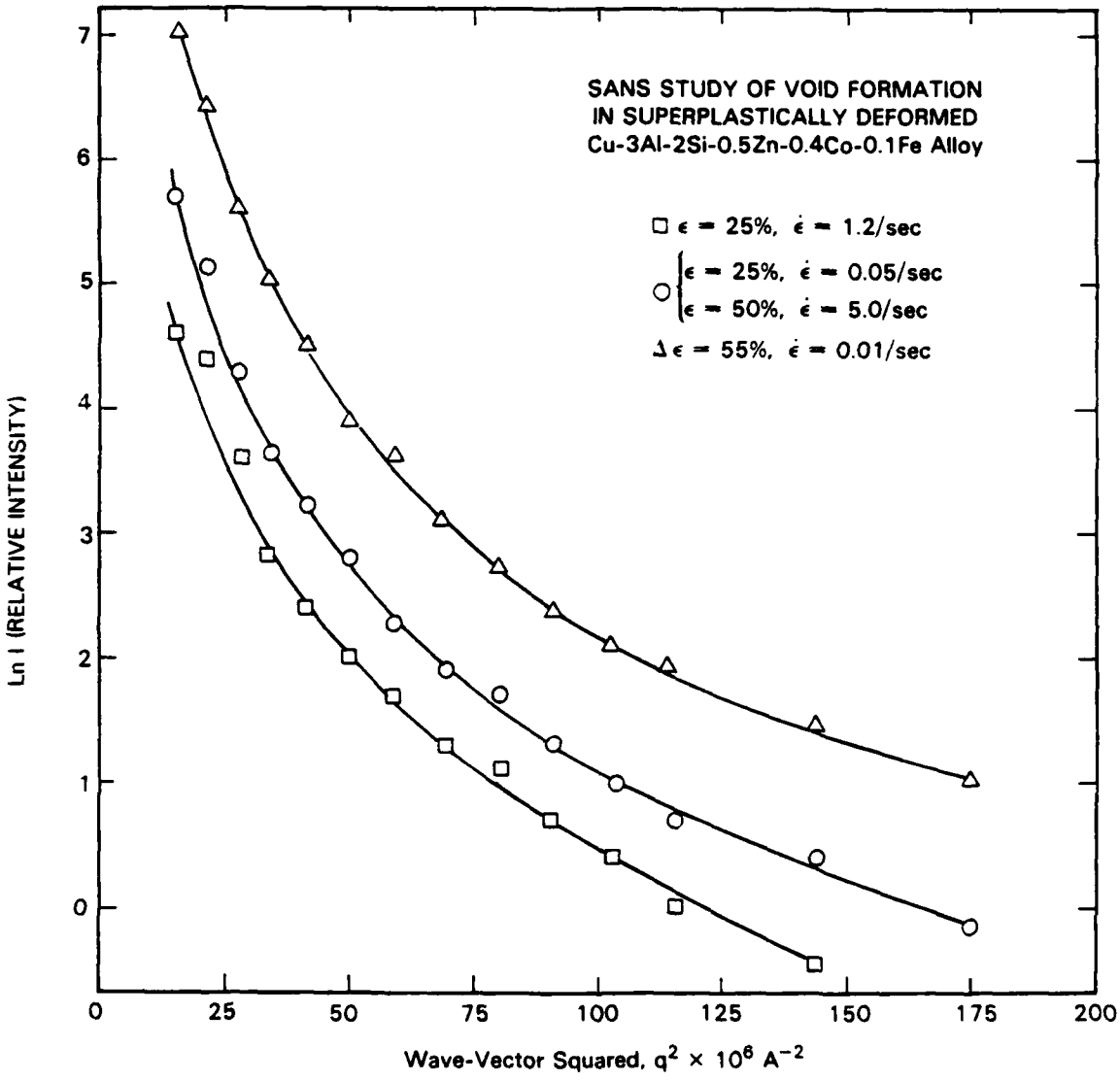

Fig. 15 — Guinier plot of SANS results from superplastically deformed Cu-3Al alloys

ACKNOWLEDGMENTS

This work has been funded in part by the Office of Naval Research and has been performed in cooperation with the National Science Foundation (Oak Ridge National Laboratory SANS Facility) and the National Bureau of Standards SANS Facility. The authors would like to thank Dr. E. Shapiro of Olin Metals Research Laboratories, Drs. J. E. Smugeresky and R. Stoltz of Sandia Corporation, and Dr. M. Dustur of Gould Corporation for supplying the needed research samples and alloys. Special thanks are due to Dr. H. R. Child of ORNL for his continued assistance in SANS measurements, Dr. C. S. Pande of the Physical Metallurgy Branch, NRL, for transmission electron microscopy, and Dr. M. A. Imam for assistance in sample preparation and helpful discussions.

REFERENCES

1. M. Fatemi and B. B. Rath, "Non-Destructive Evaluation of Defects in Structural Materials Using Long-Wavelength Neutrons," NRL Memorandum Report No. 4226, May 1980.

2. M. Fatemi, C. S. Pande, M. A. Imam, and B. B. Rath, AIME Fall 1981 Meeting, Louisville, Ky.

3. M. Fatemi and B. B. Rath, "Non-Destructive Evaluation of Defects in Structural Materials," Report to Office of Naval Research, September 20, 1980.

4. G. C. Vonk, J. Appl. Cryst., 9, 433 (1976).

5. H. A. Mook, J. Appl. Phys., 45, 43 (1974).

6. O. Glatter, J. Appl. Cryst. 13, 7 (1980).

7. I. S. Fedorova and P. W. Schmidt, J. Appl. Cryst., 11, 405 (1978).

8. A. Guinier and G. Fournet, Small-Angle Scattering of X-Rays, J. Wiley and Sons, NY (1955).

9. M. Roth, J. Appl. Cryst., 10, 172 (1977).

10. F. Nakamura et al, Phil. Mag. A 41, No. 3,307 (1980).

11. A. Guinier, Solid State Physics, Vol. 9, 336 (1958).

12. S. Shei and T. G. Langdon, Acta Metallurgica, 26, 639 (1978).

13. R. G. Fleck, C. J. Beevers and D. M. R. Taplin, Metals Science, 9, 49 (1975).

14. T. Chandra, J. J. Jones, and D. M. R. Taplin, J. Aust. Inst. Metals, 20, No. 4, 220 (1975).

END

DATE
FILMED

04-82

DTIC